HHS Public Access

Author manuscript

Biochem Biophys Res Commun. Author manuscript; available in PMC 2022 September 16.

Published in final edited form as:

Biochem Biophys Res Commun. 2011 January 28; 404(4): 928–934. doi:10.1016/j.bbrc.2010.12.083.

Dopamine D2 and D4 receptor heteromerization and its allosteric receptor-receptor interactions

Dasiel O. Borroto-Escuela[a], **Kathleen Van Craenenbroeck**[b], **Wilber Romero-Fernandez**[a], **Diego Guidolin**[c], **Amina S. Woods**[d], **Alicia Rivera**[e], **Guy Haegeman**[b], **Luigi F. Agnati**[f], **Alexander O. Tarakanov**[g], **Kjell Fuxe**[a,*]

[a]Department of Neuroscience, Karolinska Institutet, Stockholm, Sweden

[b]Laboratory of Eukaryotic Gene Expression and Signal Transduction, Ghent University, Belgium

[c]Department of Human Anatomy and Physiology, University of Padova, Italy

[d]NIDA-IRP, Structural Biology Unit, MD, USA

[e]Department of Cell Biology, Faculty of Sciences, University of Malaga, Spain

[f]IRCCS Lido Venice, Italy

[g]Russian Academy of Sciences, St. Petersburg Institute for Informatics and Automation, Russia

Abstract

Dopamine D_2 and D_4 receptors partially codistribute in the dorsal striatum and appear to play a fundamental role in complex behaviors and motor function. The discovery of D_2R–$D_{4.x}R$ ($D_{4.2}R$, $D_{4.4}R$ or $D_{4.7}R$) heteromers has been made in cellular models using co-immunoprecipitation, *in situ* Proximity Ligation Assays and BRET[1] techniques with the D_2R and $D_{4.7}R$ receptors being the least effective in forming heteromers. Allosteric receptor-receptor interactions in D_2R–$D_{4.2}R$ and D_2R–$D_{4.4}$ R heteromers were observed using the MAPK assays indicating the existence of an enhancing allosteric receptor–receptor interaction in the corresponding heteromers between the two orthosteric binding sites. The bioinformatic predictions suggest the existence of a basic set of common triplets (ALQ and LRA) in the two participating receptors that may contribute to the receptor-receptor interaction interfaces.

Keywords

Dopamine D_2R receptor; Dopamine D_4R receptor; Heteromerization; G protein-coupled receptors; Allosteric modulation; Protein-protein interactions

1. Introduction

Co-immunoprecipitation experiments suggest the existence of D_2R–D_3R heteromers in D_2R and D_3R cotransfected HEK293 cells [1]. Antiparkinsonian D_2 agonists like ropinirole and

*Corresponding author. Address: Retziusväg 8, 17177 Stockholm, Sweden. Fax: +46 8 315721., Kjell.Fuxe@ki.se (K. Fuxe).

Appendix A. Supplementary data

Supplementary data associated with this article can be found, in the online version, at doi:10.1016/j.bbrc.2010.12.083.

pramipexole appear to have a more potent effect at the D_2R–D_3R heteromer binding pockets thus the heteromer allows the D_3R to become more strongly coupled to the adenylate cyclase resulting in increased inhibition of its activity. The D_2R has also been found to form a phospholipase C-coupled heteromer with the dopamine D_1R in D_1R–D_2R cotransfected cells and both receptors co-immunoprecipitate in rat striatal membrane preparation [2]. There is evidence that the D_1R–D_2R heteromer possesses a specific coupling to the Gq/11-coupled pathway giving it a unique pharmacology with high PLC activation and low AC activation [2]. Upon coactivation of the two receptors in the D_1R–D_2R heteromer the allosteric receptor-receptor interactions may only allow the Gq/11 to couple to the D_1R–D_2R heteromer.

Dopamine D_4 receptors appear to play a fundamental role in complex behaviors mediated by the limbic system including novelty seeking behaviors and in the control and coordination of movements involving the dorsal striatum and has been postulated to form heteromers with adenosine A_{2A} receptors [3–5]. Furthermore, the D_2 and D_4 receptors partially codistribute in the dorsal striatum, especially in the matrix compartment and both of them are associated with post-synaptic elements mainly involving dendrite shafts and dendritic spines [6]. In this paper we show, for the first time, that D2 receptors can also form heteromers with three more common human dopamine $D_{4.x}R$ polymorphism variants ($D_{4.2}R$, $D_{4.4}R$ or $D_{4.7}R$) to different degrees in HEK293T cells cotransfected with human $D_{2L}R$ receptors and with any of these $D_{4.x}R$ isoforms by means of BRET[1] and *in situ* Proximity Ligation Assays (*in situ* PLA). Allosteric receptor-receptor interactions in these types of D_2R–$D_{4.x}R$ heteromers in cellular models have also been investigated using the MAPK assays.

2. Materials and methods

2.1. Plasmid constructs

The constructs presented herein ($D_{4.x}R$ and $D_{2L}R$ tagged receptor) were made using standard molecular biology techniques employing PCR and fragment replacement strategies (see Supplementary data). The other constructs used (Flag-$D_{2S}R$, HA-$D_{4.x}R$) are described previously [7].

2.2. Cell culture and transfection

HEK293T cells (American Type Culture Collection, USA) were grown in Dulbecco's modified Eagle's medium supplemented with 2 mM L-glutamine, 100 units/ml penicillin/streptomycin, and 10% (v/v) fetal bovine serum (FBS) at 37 °C and in an atmosphere of 5% CO_2. Cells were transiently transfected using linear PolyEthyleneImine reagent (PEI) (Polysciences Inc., USA).

2.3. Co-immunoprecipitation

Co-immunoprecipitation studies were performed as previously described (for more details see Supplementary data) [7].

2.4. Proximity ligation in situ assay (Duolink)

To investigate whether dopamine D_2R has the capability to interact with different isoforms of dopamine $D_{4.x}R$ we used *in situ* proximity ligation assay (PLA) [8]. *In situ* PLA was performed according to manufacturer's instructions (Duolink *in situ* PLA detection kit (Olink, Sweden)). The primary antibodies of different species directed to $D_{2L}R$ (polyclonal rabbit-anti dopamine $D_{2L}R$, Milipore) and to $D_{4.x}R$ (goat anti-dopamine $D_{4.x}R$, VitoTag Biosciences) was used. Control experiments employed only one primary antibody or cells transfected with cDNAs encoding only one type of receptor. The products were visualized using a Leica confocal microscope.

2.5. Quantitative BRET^1 assays

Quantitative BRET^1 experiments have been done as previously described (see Supplementary data) [9].

2.6. ERK1/2 phosphorylation assay

HEK293T cells transiently co-expressing $D_{2L}R$ and $D_{4.x}Rs$ were treated with the indicated concentration and times of each D_2R and D_4R agonist or antagonist and then fixed in a final concentration of 4% paraformaldehyde. After fixing, the cells were permeabilised by washing 5 times (0.1% triton-X100 in PBS), blocked for 90 min at room temperature in LI-COR Odyssey Blocking Buffer® and then incubated overnight at 4 °C with primary monoclonal mouse anti-phospho-ERK1/2 antibody (Sigma-Aldrich, Stockholm, Sweden) (diluted 1/10000). Then, after extensive wash, cells were incubated in the dark with secondary infrared probe-labeled rabbit-anti-mouse antibodies (diluted 1/1500) for 1 h at room temperature, washed and scanned by the Odyssey infrared scanner (LI-COR Biosciences).

2.7. Bioinformatic analysis of the receptor-receptor interface

Based on a bioinformatic approach, a set of amino acid triplet homologies have been deduced that may be responsible for receptor-receptor interactions among receptor heterodimers [10]. Since a significant component of the interaction interfaces leading to the assemblage of GPCR receptor dimers are intrinsically disordered domains [11], the sequences of $D_{4.x}Rs$ were also analyzed by estimating the *Disorder Index* as the weighted average of the results of seven disorder predictors for each isoform (DI, see [12]); main characteristics of which are summarized in Supplementary Tables 2–4.

2.8. Statistical analysis

The number of samples (n) in each experimental condition is indicated in figure legends. For statistical evaluation of the biochemical data, unless otherwise specified, statistical analysis was performed by one-way analysis of variance (ANOVA) followed by Tukey's Multiple Comparison post-test. The P value 0.05 and lower was considered significant.

3. Results

3.1. $D_{2L}R$ and $D_{4.x}R$ form constitutive heteromers in HEK293T cells

It has been demonstrated that dopamine D_2R form homo and heterodimers even in the absence of agonist. In order to analyze if dopamine D_2R and the most common polymorphic variants of dopamine $D_{4.x}R$ in the human population, namely $D_{4.2}R$, $D_{4.4}R$ and $D_{4.7}R$, can interact resulting in a heterodimeric complex, we used three different approaches, co-immunoprecipitation, *in situ* PLA and the BRET technology. Classic co-immunoprecipitation performed on extracts of transiently cotransfected HEK293T cells was conducted with different combinations of the three polymorphic variants of $D_{4.x}R$ and with $D_{2S}R$. As seen in Fig. 1A, the upper panel displays the immunoblot obtained with anti-HA antibodies revealing the presence and position of the HA tagged $D_{4.2}R$, $D_{4.4}R$ and $D_{4.7}R$ immunoreactive bands after immunoprecipitation of the FLAG tagged $D_{2S}R$ receptors by means of antibodies against the FLAG. The differential position of the $D_{4.2}R$, $D_{4.4}R$ and $D_{4.7}R$ immunoreactive bands is clearly seen, demonstrating co-immunoprecipitation of the $D_{4.2}R$, $D_{4.4}R$ and $D_{4.7}R$ with the $D_{2S}R$. In the lower panel the immunoblot obtained with the anti-FLAG antibodies also shows the presence of the FLAG tagged $D_{2S}R$ in the four lanes after the anti-FLAG immunoprecipitation. Proper expression of the constructs was confirmed by Western blots with their respective anti-HA and anti-FLAG antibodies performed on total cell lysates (left panel of Fig. 1A).

3.2. In situ PLA detection of $D_{2L}R$ and $D_{4.x}R$ physical interaction in HEK293T cells

For *in situ* detection of $D_{2L}R$ and $D_{4.x}R$ ($D_{4.2}R$, $D_{4.4}R$ or $D_{4.7}R$) heteromers, a version of the PLA technique was applied using unconjugated primary antibodies from different species, one recognizing D_2R (rabbit anti-D_2R) and the other recognizing D_4R (goat anti-D_4R), which are detected by secondary antibodies covalently coupled to oligonucleotides, the so-called proximity MINUS and PLUS probes. Only when both primary and secondary antibodies are bound to their respective target molecules can proximity-dependent ligation and rolling circle amplification of a circular DNA reporter molecule occur (Fig. 1B). Subsequent hybridization of complementary red fluorescence-labeled oligonucleotides to the rolling circle amplification visualized the PLA-detected $D_{2L}R$–$D_{4.x}R$ interactions as red clusters (blobs) (Fig. 1C). Specificity was demonstrated by the failure of seeing red clusters over the nuclei and their absence after omitting either one of the antibodies. Furthermore, the fluorescent labelled oligonucleotides did not cause the appearance of red clusters unless the amplification procedure had been performed (data not shown). PLA positive red clusters are found mainly located along the surface membrane of the cells following all combinations of receptor co-expression ($D_{2L}R$–$D_{4.x}R$). The lowest number of red clusters (blobs) was found after cotransfection with $D_{2L}R$ and $D_{4.7}R$. The low number of PLA signals detected for $D_{2L}R$–$D_{4.7}R$ in these cell lines was not due to a variable receptor expression level as receptor level expression was almost equal for each receptor pair co-expressed. In summary, these results are consistent with our co-immunoprecipitation results and indicated that D_2R–$D_{4.x}R$ form heteromers.

3.3. Study of $D_{2L}R$ and $D_{4.x}R$ heteromerization in HEK293T cells by BRET[1] assays

To further characterize the heterodimeric interactions of dopamine $D_{4.x}R$ polymorphic variants and dopamine D_2R we examined the possibility of direct receptor-receptor interactions by constructing quantitative BRET saturation curves in cells transiently co-transfected with a constant amount of $D_{4.2}R$-Rluc, $D_{4.4}$-Rluc or $D_{4.7}$-Rluc construct and increasing concentrations of the $D_{2L}R$-YFP plasmids. Although BRET isotherm curves generated by fluorescence- and luminescence-directed measurements provide the theoretical behavior sufficient to predict receptor heterodimers, this analysis does not take in account the receptor expression level required for a proper quantitative analysis of receptor-receptor interactions. In view of which, we conducted saturation experiments in which the amount of each receptor effectively expressed in transfected cells was monitored for each individual experiment by correlating both total luminescence and total fluorescence with the receptor densities (fmol/mg total protein, Supplementary M&M and Fig. 1). The linear regression equations derived from “Supplementary material” were thus used to transform the luminescence and fluorescence values into receptor number. BRET signals were plotted as a function of the ratio between the receptor-YFP/receptor-Rluc numbers.

As shown in Fig. 2A and B, significant quantitative BRET signals were found for the $D_{2L}R$–$D_{4.2}R$ and $D_{2L}R$–$D_{4.4}R$ pairs, giving also the highest maximum BRET values ($BRET_{max}$). A substantially lower $BRET_{max}$ signal was obtained with the $D_{2L}R$–$D_{4.7}R$ pair which was also shown to possess a significantly higher $BRET_{50}$ value (Fig. 2B). In all cases, BRET increased as a hyperbolic function of the increasing concentration of the YFP fusion construct, reaching an asymptote at the highest concentrations used. To test that the BRET signal was indeed a result of a specific protein–protein interaction, we performed two essential control experiments. First, we co-expressed the $D_{2L}R$-Rluc with soluble YFP which indeed led to marginal signals that increased linearly with increasing amounts of YFP expressed (Fig. 2A and B). Secondly, we over-expressed increasing concentrations of WT receptor (Supplementary Fig. 2) in combination with the protomers of the BRET pair (constant ratio 1:1) and investigated whether the WT receptor could reduce the BRET signal. Over-expression of the WT receptor significantly reduced the BRET ratio, as shown in the BRET competition curves in Supplementary Fig. 2.

The existence of $D_{4.x}R$ homomers has also been studied and compared with $D_{2L}R$ homomers (Supplementary Fig. 3). In contrast to the results obtained with the D_2R–$D_{4.x}R$ heteromers similar $BRET_{max}$ values were found with $D_{4.2}R$, $D_{4.4}R$ and $D_{4.7}R$ homomers (only small reduction in the $BRET_{max}$ for the $D_{4.7}R$ homomer). However, the $D_{4.7}R$ homomer had significantly reduced $BRET_{50}$ value vs the $D_{4.2}R$ and $D_{4.4}R$ homomers. When comparing the BRET saturation curves obtained for the $D_{2L}R$, $D_{4.2}R$ and $D_{4.4}R$ homo- and heterodimers (Supplementary Table 1), similar $BRET_{50}$ values for the heteromers were obtained, indicating that the receptors had similar relative affinities to one another. However, the $BRET_{50}$ of $D_{4.7}R$ homodimers showed a significantly higher affinity with respect to the $D_{2L}R$–$D_{4.7}R$ heterodimer and $D_{2L}R$, $D_{4.2}R$ and $D_{4.4}R$ homo- and heterodimers. This has important implications, since it suggests that, under basal conditions, $D_{4.7}R$ homo- and heterodimers have a different probability of forming when the two receptors are heterologously expressed. Instead, it is very probable that $D_{4.7}R$ receptor subtypes may

form mainly homodimers when they are co-expressed with other $D_{4.x}R$ isoforms or D_2R subtypes.

3.4. Structural determinants potentially involved in hetero- vs homooligomerization based on bioinformatic analysis

Based on a bioinformatics approach, Tarakanov and Fuxe [10] have deduced a set of triplet homologies that may be responsible for receptor-receptor interactions. This set consists of two non-intersecting subsets: 'pro-triplets' and 'contra-triplets'. Any protriplet appears as a homology in at least one heterodimer but does not appear as a homology in any non-heterodimer. Just the reverse, any contra-triplet appears in at least one non-heterodimer but does not appear in any heterodimer. In the $D_{2L}R–D_{4.x}R$ heteromer two pro-triplets has been identified; ALQ in the first intracellular loop of both receptor protomers and the LRA in the third intracellular loop (IL3) of $D_{2L}R$ and C-terminal tail of $D_{4.x}R$ (Fig. 3A and Supplementary Fig. 4). The triplet of amino acid residues ALQ (Ala-Leu-Gln) appears as a homology in one more receptor heterodimer: $D_2R–D_3R$, whereas the triplet LRA (Leu-Arg-Ala) appears as a homology in two more heterodimers: D_2R-NTS1 and TLR1-TLR2. Moreover, the triplets ALQ and LRA may play a role in the HIV entry and the repeat proteins [10]. Taken together with the BRET experimental results, these bioinformatic predictions suggest the existence of two sets of common triplets in the two participating receptors that may contribute in the receptor-receptor interaction interfaces.

The analysis of the intrinsic disorder in $D_{4.x}R$ provided a high mean disorder index in the IL3 for all the analyzed isoforms of the receptor, suggesting a potential significant role of this domain in receptor-receptor interactions involving $D_{4.x}R$. As shown in Fig. 3B, if the size of IL3 is also taken into consideration (by estimating an *Integrated Disorder Index* as the product of the mean DI and the number of AA forming the domain) a significant difference between $D_{4.7}R$ and the other $D_{4.x}R$ isoforms can be observed. Thus, this bioinformatics analysis is consistent with the possibility of a different behavior of the three alleles as far as receptor-receptor interactions are concerned.

3.5. Functional consequences of $D_{2L}R–D_{4.x}R$ heteromerization on ERK1/2 phosphorylation

The receptor-receptor interactions within the $D_{2L}R–D_{4.x}R$ heteromers were studied by analysis of ERK1/2 phosphorylation after selective D_2R (quinerolane) and D_4R (PD168077) agonist treatment and their combination in $D_{2L}R–D_{4.2}R$, $D_{2L}R–D_{4.4}R$ and $D_{2L}R–D_{4.7}R$ cotransfected cells. When $D_{2L}R$ and $D_{4.x}R$ were expressed alone; selective agonist activation of $D_{2.2}R$ and $D_{4.4}R$ (with agonist concentrations 3 times the Ki values (50 nM)) produced a somewhat more short-term activation over a period of 10 min while selective agonist activation of $D_{4.7}R$ and $D_{2L}R$ produced a somewhat prolonged response (20 min) in terms of MAPK activation (Supplementary Fig. 5A). The time course experiments of co-expressing cells are shown in Fig. 4A. Both the D_2R and D_4R agonists produced a rise of ERK1/2 phosphorylation with combined treatment resulting in additive actions. It is of substantional interest that in the $D_{2L}R–D_{4.7}R$ unlike $D_{2L}R–D_{4.2}R$ and $D_{2L}R–D_{4.4}R$ co-expressing cells no additive effects could be observed on the MAPK activity (Fig. 4A). Thus, indications are obtained that allosteric receptor-receptor interactions are different

in $D_{2L}R$–$D_{4.7}R$ heteromers not allowing the D_4R agonist to produce any further effect on ERK1/2 phosphorylation compared with the one produced by the D_2R agonist in this heteromer.

The D_4R agonist modulation of the D_2R agonist concentration-response curve in $D_{2L}R$–$D_{4.2}R$, $D_{2L}R$–$D_{4.4}R$ and $D_{2L}R$–$D_{4.7}R$ cotransfected cells is displayed in Fig. 4B. We can observe that the D_4R agonist shifts the D_2R agonist concentration-response of ERK1/2 phosphorylation to the left in the case of $D_{2L}R$–$D_{4.2}R$, $D_{2L}R$–$D_{4.4}R$ but not $D_{2L}R$–$D_{4.7}R$ cotransfected cells. Thus, an enhancing $D_{4.x}R$–$D_{2L}R$ interaction may exist in the $D_{2L}R$–$D_{4.2}R$, $D_{2L}R$–$D_{4.4}R$ cells with $D_{4.x}R$ activation potentially increasing the affinity of the $D_{2L}R$ agonist binding sites.

The detailed pharmacological analysis is shown in Supplementary Fig. 5B and C with selective D_2R (L741–626) and D_4R antagonists (L641–642) counteracting the rises of the ERK1/2 phosphorylation produced by D_2R and D_4R agonists in $D_{2L}R$ and $D_{4.x}R$ alone and co-expressing cells, respectively.

4. Discussion

Evidence is presented with the PLA method that in HEK293 cells $D_{2L}R$ can form heteromers with $D_{4.7}R$ and especially with $D_{4.2}R$ and $D_{4.4}R$ located mainly along the plasma membrane seen as PLA positive red clusters (blobs). The specificity was seen from the absence of these clusters when only one type of DA receptors was transfected into the HEK293 cells or when only one of the DA receptor antibodies was employed. Evidence was also obtained with the $BRET^1$ technique that $D_{2L}R$ can form heteromers with $D_{4.2}R$, $D_{4.4}R$ and $D_{4.7}R$, the $D_{4.7}R$ being the least capable one as seen from the reduced $BRET_{max}$ and increased $BRET_{50}$ values compared with those obtained with the $D_{4.2}R$ and $D_{4.4}R$ protomers in line with the results using the PLA method. Specificity is assigned in the BRET competition assays. The PLA and $BRET^1$ results were strongly supported by the results from the co-immunoprecipitation experiments. In the immunoblot with the antibodies against the HA tag of the $HAD_{4.x}R$ constructs the co-immunoprecipitated $D_{4.x}R$ isoforms could clearly be distinguished after immunoprecipitation of the FLAG $D_{2S}R$construct with the antibody of its FLAG tag.

The functional consequences of the different types of D_2R-$D_{4.x}R$ heteromers formed were evaluated in the MAPK assay using selective D_2R (quinerolane) and D_4R agonists (PD) and their combination.

Combined treatment resulted in additive effects on ERK1/2 phosphorylation for $D_{4.2}R$, $D_{4.4}R$ but not for $D_{4.7}R$ containing heteromers with the other protomer being $D_{2L}R$. Thus, the integrated signal of MAPK was different in the $D_{2L}R$–$D_{4.7}R$ heteromers with a failure of the D_4R agonist to produce additive effects on the D_2R agonist induce ERK1/2 phosphorylation. $D_{4.2}R$ and $D_{4.4}R$ had a more rapid onset of ERK1/2 phosphorylation and disappearance upon D_4R agonist treatment alone than $D_{4.7}R$ which upon D_4R agonist activation had a similar prolonged time-course as found with D_2R agonist induced activation of the $D_{2L}R$ alone. This temporal profile existed at $D_{4.7}R$ both as a homomer and as

heteromer with $D_{2L}R$. The most interesting findings were obtained in the D_4R agonist modulation of the ERK phosphorylation concentration-response curves to the D_2R agonist at the 10 min time-interval testing the MAPK signaling of the three types of D_2R–$D_{4.x}R$ heteromers demonstrated in this study. Upon D_4R agonist activation of the $D_{4.2}R$ and $D_{4.4}R$ the concentration-response curve was shifted to the left, which was not the case after agonist activation of the $D_{4.7}R$. Thus, the D_2R protomer appears to develop an increased affinity of their agonist binding sites after agonist activation of the $D_{4.2}R$ and $D_{4.4}R$ protomer of the heteromer indicating the existence of an enhancing allosteric receptor–receptor interaction in the corresponding heteromers between the two orthosteric binding sites. This receptor-receptor interaction does not appear to develop between the $D_{4.7}R$ and $D_{2L}R$ upon D_4R agonist activation implying that many tandem repeats in the $D_{4.x}R$ may alter the development of the allosteric receptor-receptor interaction in a heteromer built up of $D_{4.7}R$ and $D_{2L}R$. This may also help explain the failure to see additive effects on MAPK activity after combined treatment of D_2R and D_4R agonist at $D_{2L}R$–$D_{4.7}R$ heteromers. It may be that this deficit in the allosteric D_2R–$D_{4.7}R$ interaction is linked to a reduced ability of these two DA receptors to form heteromers as judged from the PLA and $BRET^1$ assays. It should also be noted that the size of the disordered regions is significantly increased in intracellular loop 3 of $D_{4.7}R$ which may increase its ability to form homomers and reduce its ability to form heteromers with $D_{2L}R$.

In terms of homomers of $D_{4.2}R$, $D_{4.4}R$ and $D_{4.7}R$ as studied with the $BRET^1$ technique the rank order among them was different compared with the heteromers they formed with $D_{2L}R$ (see above). In the case of homomer formation the $D_{4.7}R$ showed an increased affinity (reduced $BRET_{50}$) compared with $D_{4.2}R$ and $D_{4.4}R$ while the opposite was true for the formation of the respective heteromers (see above). Also there were no clear-cut differences among the tandem repeats of $D_{4.x}R$ studied with regard to the $BRET^1_{max}$ values obtained in homomer formation. It therefore seems that $D_{4.2}R$ and $D_{4.4}R$ more easily form heteromers with $D_{2L}R$-while $D_{4.7}R$ may favor the formation of homomers over heteromerization with $D_{2L}R$.

Taken together, $D_{2L}R$–$D_{4.x}R$ heteromers have been demonstrated in cellular models and their integrated signaling at the MAPK is different in the $D_{2L}R$–$D_{4.7}R$ heteromers vs the other two heteromers. It is postulated that these novel D_2R–$D_{4.x}R$ heteromers play a role in the forebrain.

Supplementary Material

Refer to Web version on PubMed Central for supplementary material.

Acknowledgments

This work was supported by grants from the Swedish Research Council (04X-715), Hjärnfonden, Torsten and Ragnar Söderberg and M.M. Wallenberg Foundation to K.F. K.V.C. has a postdoctoral fellowship from FWO. A.O.T. has not received any support for this work. This research was supported in part by the Intramural Research Program of the National Institute on Drug Abuse, NIH.

References

[1]. Scarselli M, Novi F, Schallmach E, Lin R, Baragli A, Colzi A, Griffon N, Corsini GU, Sokoloff P, Levenson R, Vogel Z, Maggio R, D2/D3 dopamine receptor heterodimers exhibit unique functional properties, J. Biol. Chem 276 (2001) 30308–30314. [PubMed: 11373283]

[2]. Rashid AJ, O'Dowd BF, Verma V, George SR, Neuronal Gq/11-coupled dopamine receptors: an uncharted role for dopamine, Trends Pharmacol. Sci 28 (2007) 551–555. [PubMed: 17950471]

[3]. Rubinstein M, Phillips TJ, Bunzow JR, Falzone TL, Dziewczapolski G, Zhang G, Fang Y, Larson JL, McDougall JA, Chester JA, Saez C, Pugsley TA, Gershanik O, Low MJ, Grandy DK, Mice lacking dopamine D4 receptors are supersensitive to ethanol, cocaine, and methamphetamine, Cell 90 (1997) 991–1001. [PubMed: 9323127]

[4]. Dulawa SC, Grandy DK, Low MJ, Paulus MP, Geyer MA, Dopamine D4 receptor-knock-out mice exhibit reduced exploration of novel stimuli, J. Neurosci 19 (1999) 9550–9556. [PubMed: 10531457]

[5]. Fuxe K, Ferre S, Canals M, Torvinen M, Terasmaa A, Marcellino D, Goldberg SR, Staines W, Jacobsen KX, Lluis C, Woods AS, Agnati LF, Franco R, Adenosine A2A and dopamine D2 heteromeric receptor complexes and their function, J. Mol. Neurosci 26 (2005) 209–220. [PubMed: 16012194]

[6]. Rivera A, Cuellar B, Giron FJ, Grandy DK, de la Calle A, Moratalla R, Dopamine D4 receptors are heterogeneously distributed in the striosomes/matrix compartments of the striatum, J. Neurochem 80 (2002) 219–229. [PubMed: 11902112]

[7]. Rondou P, Haegeman G, Vanhoenacker P, Van Craenenbroeck K, BTB Protein KLHL12 targets the dopamine D4 receptor for ubiquitination by a Cul3-based E3 ligase, J. Biol. Chem 283 (2008) 11083–11096. [PubMed: 18303015]

[8]. Soderberg O, Gullberg M, Jarvius M, Ridderstrale K, Leuchowius KJ, Jarvius J, Wester K, Hydbring P, Bahram F, Larsson LG, Landegren U, Direct observation of individual endogenous protein complexes in situ by proximity ligation, Nat. Methods 3 (2006) 995–1000. [PubMed: 17072308]

[9]. Borroto-Escuela DO, Garcia-Negredo G, Garriga P, Fuxe K, Ciruela F, The M(5) muscarinic acetylcholine receptor third intracellular loop regulates receptor function and oligomerization, Biochim. Biophys. Acta 1803 (2010) 813–825. [PubMed: 20398705]

[10]. Tarakanov AO, Fuxe KG, Triplet puzzle: homologies of receptor heteromers, J. Mol. Neurosci 41 (2010) 294–303. [PubMed: 19960372]

[11]. Guidolin D, Ciruela F, Genedani S, Guescini M, Tortorella C, Albertin G, Fuxe K, Agnati LF, Bioinformatics and mathematical modelling in the study of receptor-receptor interactions and receptor oligomerization Focus on adenosine receptors, Biochim. Biophys. Acta (2010), doi:10.1016/j.bbamem.2010.09.022.

[12]. Agnati LF, Leo G, Genedani S, Andreoli N, Marcellino D, Woods A, Piron L, Guidolin D, Fuxe K, Structural plasticity in G-protein coupled receptors as demonstrated by the allosteric actions of homocysteine and computer-assisted analysis of disordered domains, Brain Res. Rev 58 (2008) 459–474. [PubMed: 18022243]

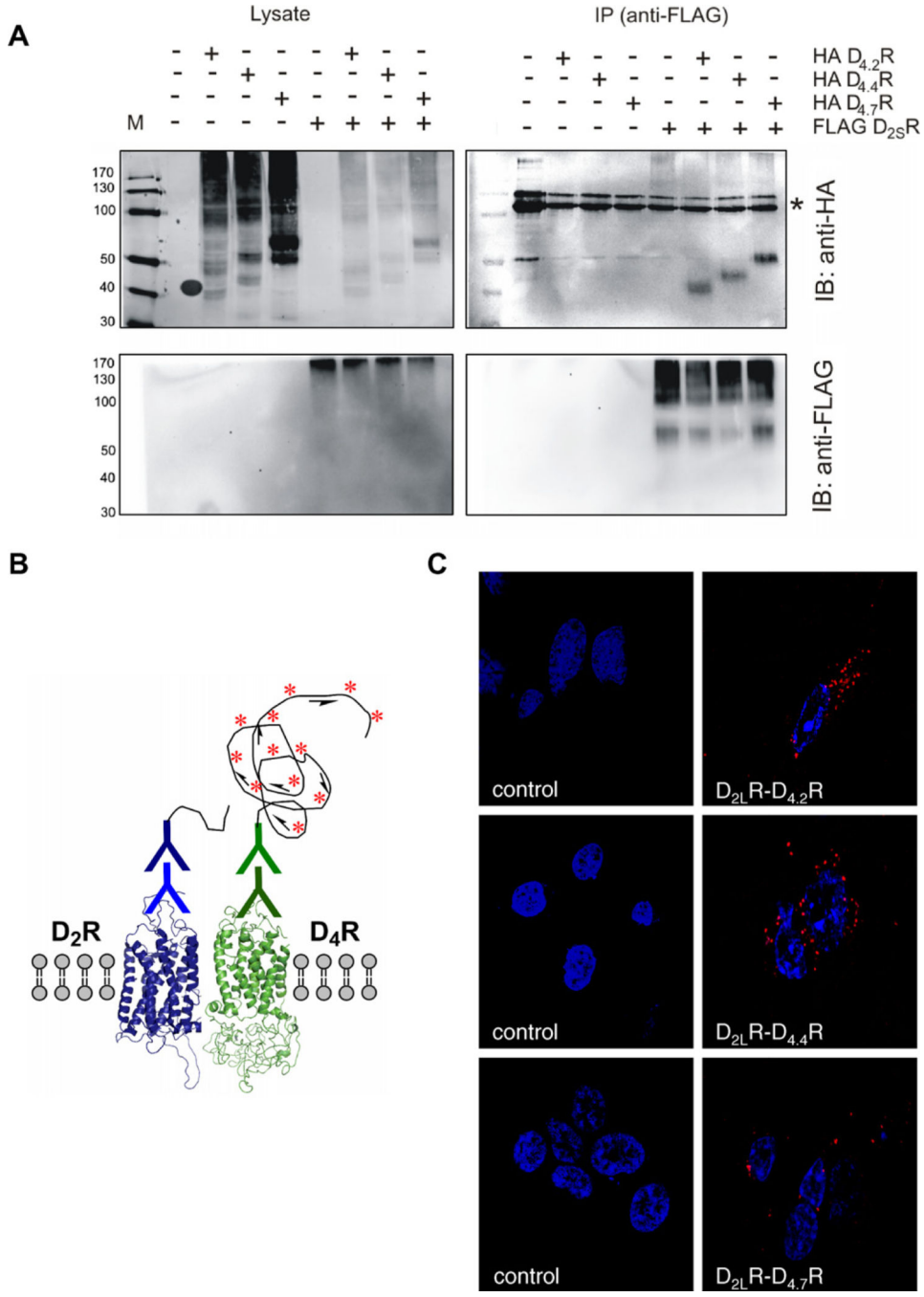

Fig. 1.

Dopamine D_2R and the different polymorphic variants of dopamine $D_{4.x}R$ form constitutive heteromers. Representative images were obtained in co-immunoprecipitation experiments and *in situ* PLA. (A) Co-immunoprecipitation studies of $FLAGD_{2S}R$ and $HAD_{4.2/4.4/4.7}R$ were performed in HEK293T cells. Immunoprecipitation (IP) was made with mouse anti-FLAG (M2) antibody (2 μg). Proteins were visualized with HRP-coupled anti-FLAG M2 or rabbit anti-HA (lysates) or mouse anti-HA (16B12) (IP blot) antibody (1/1000) and HRP-coupled anti-mouse (1/2000). Signal denoting anti-FLAG antibody is indicated

with (*). (B) Schematic representation of *in situ* PLA detection. Blue and green is indicate the primary and oligo-conjugated secondary antibodies. The long curved black line represents the circular DNA template that resulted from proximity-dependent ligation and was amplified by rolling circle amplification. The fluorescent-oligonucleotide detection probes are represented by red-asterisk. (C) HEK293T cells were transiently transfected with $D_{2L}R$ and $D_{4.x}R$ and grown as described in Section 2. After fixation, *in situ* PLA was performed with D_2R and D_4R-specific antibodies, followed by PLA reagents. The detected heterodimers are represented by the fluorescent rolling circle products (red clusters). Nuclei are shown in blue (DAPI). (For interpretation of the references to color in this figure legend, the reader is referred to the web version of this article.)

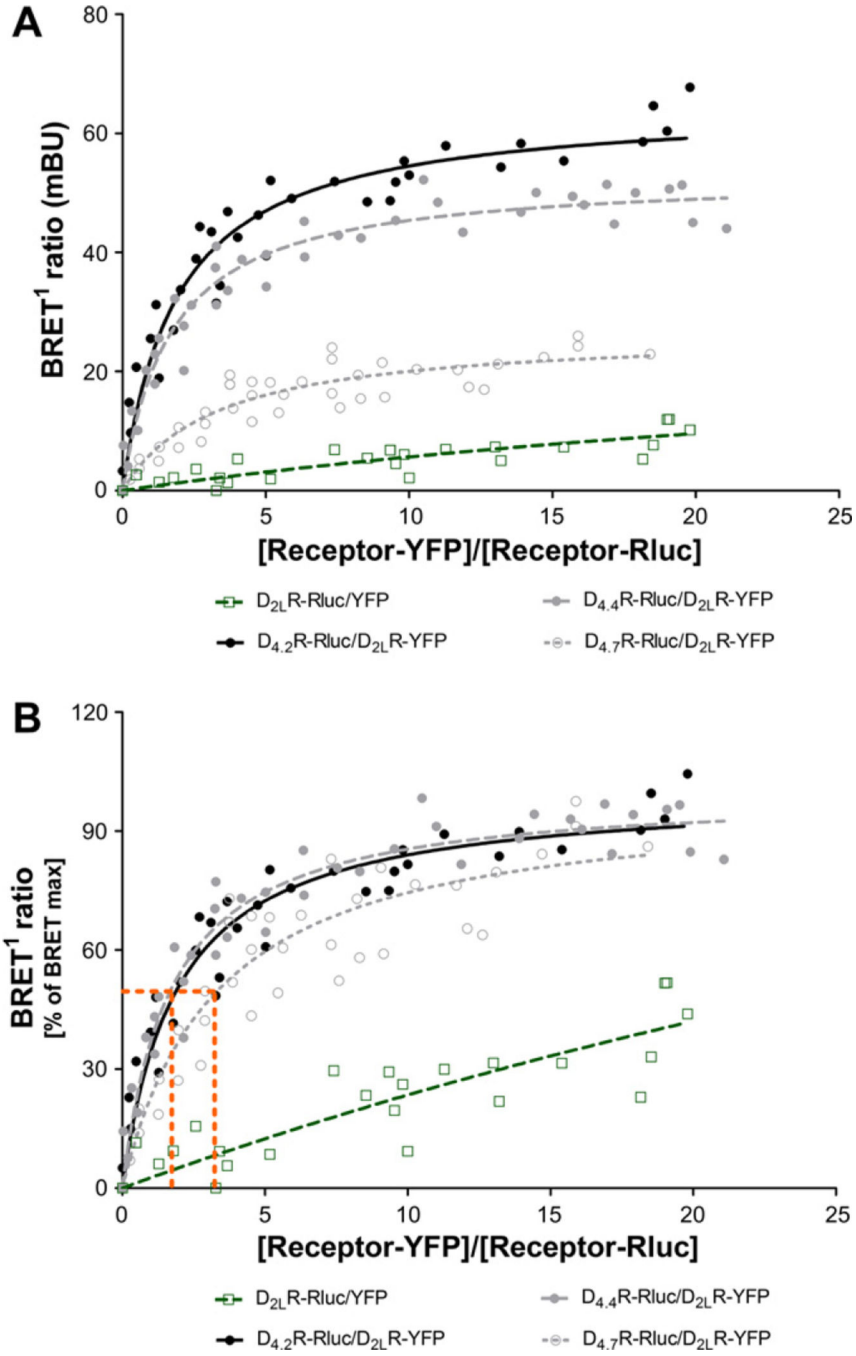

Fig. 2.

Quantitative analysis of $D_{2L}R$ and $D_{4.x}R$ heterodimerization. $BRET^1$ donor saturation curves were performed by transfecting HEK293T cells with a constant DNA concentration of acceptor receptor-Rluc and increasing concentrations of donor receptor-YFP constructs. $BRET^1$ ratio, total fluorescence, and total luminescence as well as transformed values into receptor numbers were determined as described under supplementary material. The curves represent 8 saturation curves that were fitted using a non-linear regression equation assuming a single binding site.

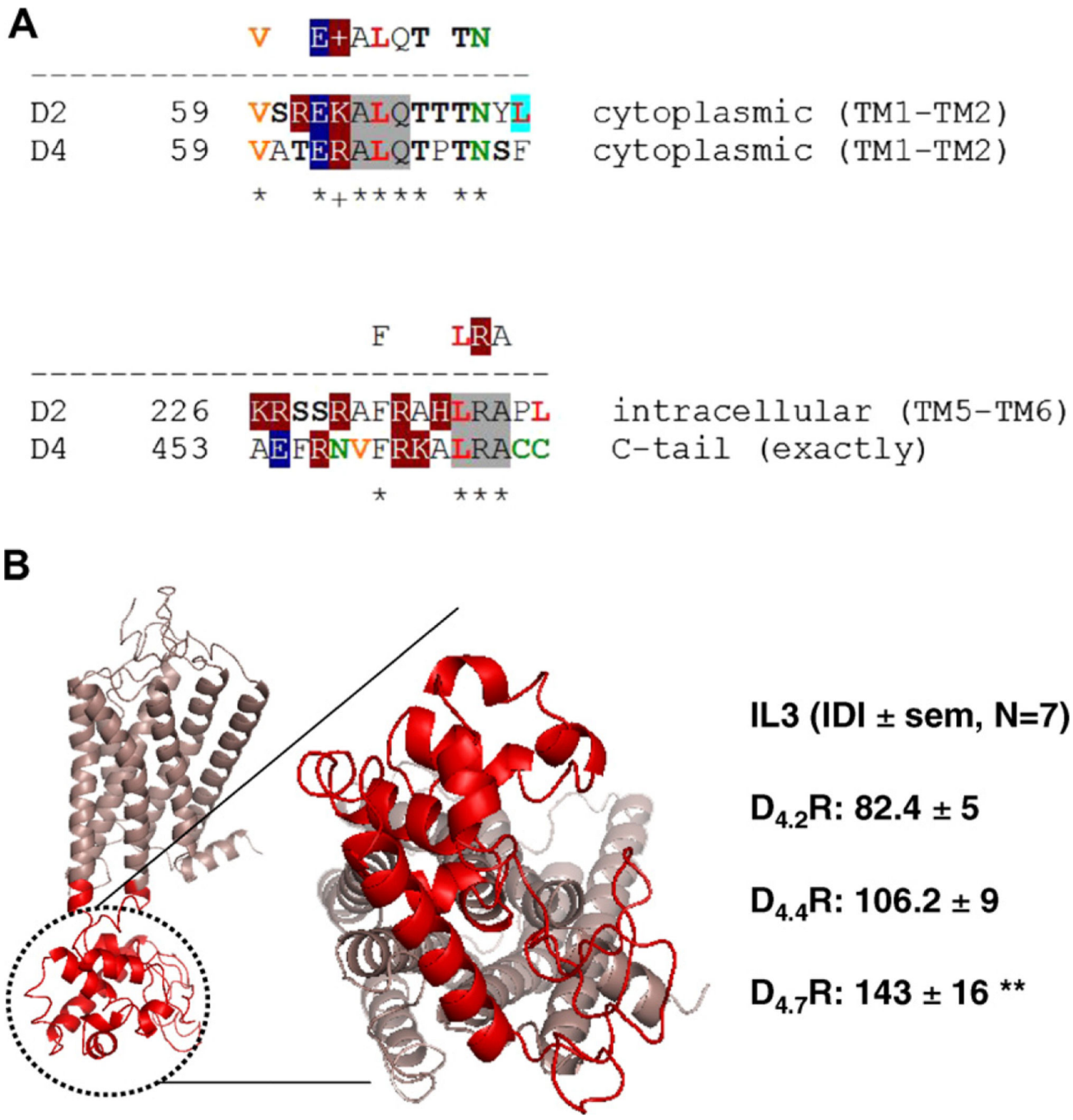

Fig. 3.

(A) Bioinformatic analysis and sequence alignment of $D_{4.x}R$ and D_2R receptor homologies containing the triplet homologies ALQ (in the IL1 in both receptors) and LRA (in the IL3 and C-tail of D_2R and $D_{4.x}R$, respectively) in the receptor interface. The following amino acid residues are marked by a color code as the basic elements of leucine-rich motifs. Red bold, (Leu). Orange bold, (Ile) and (Val) that may also occupy a position of Leu in leucine-rich motifs. Green, (Asn) and (Cys). Black bold, (Ser) and (Thr) where agonist-regulated phosphorylation may occur. White letters are charged amino acids: negatively charged (dark

blue background) (Glu), (Asp) or positively charged (dark red background) (Arg), (Lys), (His). Color-shaded are two-letter homologies which include leucine and seem rather typical for ligand-receptor interactions: LL (green), LI or IL and LV or VL (blue), LN (pink), together with 'leucine-serine zipper' LSS, LS or SL (yellow). (B) Per-residue analysis of the intrinsic disorder in $D_{4.x}R$. The molecular model of $D_{4.4}R$ is represented (in red the lateral and cytosolic views of IL3) Each amino acids (aa) was assigned a *Disorder Index* value as the ratio between the number of predictors estimating it as belonging to a disordered sequence and the total number of predictors used. Thus, this value ranges between 0 (no predictor estimated the aa as 'disordered') and 1 (all the predictors estimated the aa as 'disordered'). (For interpretation of the references to color in this figure legend, the reader is referred to the web version of this article.)

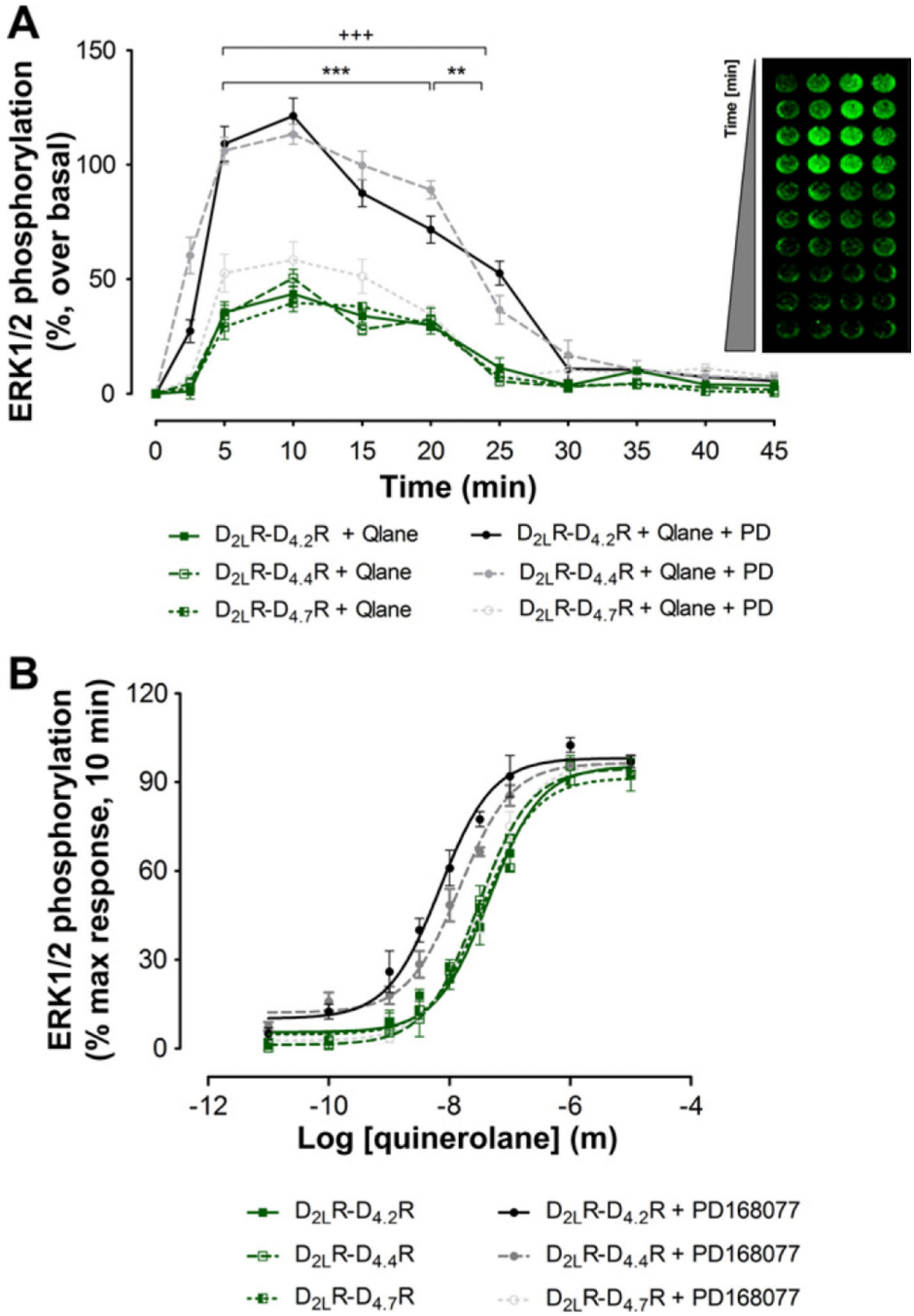

Fig. 4.

Functional consequences of $D_{2L}R–D_{4.x}R$ heteromerization on ERK1/2 phosphorylation. (A) An *in cell western* assay was used to measure ERK1/2 phosphorylation in HEK293T cells co-expressing $D_{4.x}R$ and D_2R receptors and treated in presence or absence of D_2R and D_4R receptor selective agonists (quinerolane, 50 nM and PD168077 (PD), 50 nM) in the time frame of 0–45 min. Similar experiments were carried out without stimulation (vehicle). The data represent the mean ± SEM; $n = 3$ in quadruplicate. Combined quinerolane and PD168077 $D_{2L}R–D_{4.2}R$ is significantly different compared to quinerolane $D_{2L}R–D_{4.2}R$ in

the range of 5–25 min (+++: $P < 0.001$). Combined quinerolane and PD168077 $D_{2L}R$–$D_{4.4}R$ is significantly different compared to quinerolane $D_{2L}R$–$D_{4.4}R$ in the range of 5–20 min (***: $P < 0.001$) and 20–25 min (**: $P < 0.01$), by two-way analysis of variance (ANOVA). (B) Concentration-response curve of quinerolane induced ERK1/2 phosphorylation. Cells co-expressing D_2R and $D_{4.x}R$ were stimulated in presence or absence of the D_4R selective agonist PD168077 (100 nM) during 10 min. PD168077 at 100 nM shifts the concentration-response curve of quinerolane on ERK1/2 phosphorylation to the left in cells co-expressing only $D_{2L}R$–$D_{4.2}R$ and $D_{2L}R$–$D_{4.4}R$. Data represent the mean ± SEM; $n = 3$ in triplicate. Qlane: quinerolane.